

Strange matter and strange stars in a thermodynamically self-consistent perturbation model with running coupling and running strange quark mass

J. F. Xu,¹ G. X. Peng,^{1,2,*} F. Liu,³ De-Fu Hou,³ and Lie-Wen Chen⁴

¹*School of Physics, University of Chinese Academy of Sciences, 380 Huaibeizhen, Beijing 101408, China*

²*Theoretical Physics Center for Science Facilities, Institute of High Energy Physics, Beijing 100049, China*

³*Key Laboratory of Quark & Lepton Physics (MOE) and Institute of Particle Physics, Central China Normal University, Wuhan 430079, China*

⁴*Department of Physics and Astronomy and Shanghai Key Laboratory for Particle Physics and Cosmology, Shanghai Jiao Tong University, Shanghai 200240, China*

(Received 21 April 2015; published 17 July 2015)

A quark model with running coupling and running strange quark mass, which is thermodynamically self-consistent at both high and lower densities, is presented and applied to study properties of strange quark matter and structure of compact stars. An additional term to the thermodynamic potential density is determined by meeting the fundamental differential equation of thermodynamics. It plays an important role in comparatively lower density and ignorable at extremely high density, acting as a chemical-potential dependent bag constant. In this thermodynamically enhanced perturbative QCD model, strange quark matter still has the possibility of being absolutely stable, while the pure quark star has a sharp surface with a maximum mass as large as about 2 times the solar mass and a maximum radius of about 11 kilometers.

DOI: [10.1103/PhysRevD.92.025025](https://doi.org/10.1103/PhysRevD.92.025025)

PACS numbers: 21.65.Qr, 05.70.Ce, 12.38.Bx, 12.39.-x

I. INTRODUCTION

In recent decades, strange quark matter (SQM) has been one of the most interesting and significant topics in nuclear physics [1]. Early in the 1970s, the possible existence of a deconfined phase was proposed and studied [2–5]. Especially in 1984, it was speculated, based on elementary symmetry considerations, that SQM might be absolutely stable and thus have important consequences [6]. Soon after this it was shown in the MIT bag model that SQM is absolutely stable for a reasonable range of QCD-related parameters [7]. Since then many papers have been done on the properties and applications [8–22].

It is widely believed that quantum chromodynamics (QCD) is the fundamental theory of strong interactions, and in principle, one could do a detailed and comprehensive study on SQM by solving the motion equations of quarks and gluons. Unfortunately, however, QCD is, in fact, intractable in the nonperturbative regime presently. In particular at finite baryon chemical potential, there is a notorious sign problem where the lattice Monte Carlo simulation is inaccessible [23]. Therefore, effective phenomenological models play crucial roles to extract and figure out the properties of strongly interacting matter. In past years, a number of models have been applied with interesting results, such as the Nambu-Jona-Lasinio model [24,25], the global color symmetry model [26], the quasiparticle model [27–33], the mass-density-dependent model

[34–39], the equiparticle model [40,41], the quark-cluster model [42], and so on.

Thermodynamic consistency is a fundamental requirement of phenomenological models [38]. In many important cases, an additional term to the thermodynamic potential density is necessary to maintain thermodynamic consistency. In an important version of the quasiparticle model, for example, the additional term is needed in both the zero [43] and finite temperature [44] cases. In the equiparticle model with confinement by the density dependence of quark masses, an additional term also appears in the thermodynamic potential density to have full thermodynamic consistency [40,41].

Because of asymptotic freedom, the perturbative calculation of QCD is reliable at very high densities. The thermodynamic potential density of cold quark matter was calculated for massless quarks in Refs. [45–47]. These results were applied to study quark stars to the first order in QCD coupling in Refs. [48,49], to the second order in [50], with finite-mass effect of strange quarks considered in Refs. [51–53].

The validity of a perturbative theory requires a small coupling with which the perturbative series is obtained. Different from quantum electrodynamics (QED), however, the QCD coupling is running, i.e., it is not that small when the density is not extremely high. In this case, one will meet thermodynamic problem when one naively extends the applicable range of density [54].

One way to solve this problem is to add an additional term to the thermodynamic potential density, similar to that of the popular quasiparticle model [55–58] and the

*Corresponding author.
gxpeng@ucas.ac.cn

equivparticle model [40,41]. This way of extending the applicable range of the perturbative calculation was shown to be reasonable for the one-flavor case [54]. It has also been shown, for the massless two-flavor case, that the renormalization subtraction point should be taken as a function of the summation of the biquadratic chemical potentials while the additional term not only keeps the thermodynamics self-consistent, but also produces reasonable results [59]. In the present paper, we extend this thermodynamically enhanced perturbative QCD (EPQ) model to the actual SQM with massless up (u) and down (d) quarks plus massive strange (s) quarks. It is found that the additional term takes an important role at lower densities, acting as a chemical-potential dependent bag constant. The equation of state (EOS) of SQM becomes stiffer, and accordingly the maximum mass of strange stars is as large as 2 times the solar mass.

The paper is organized as follows. In Sec. II, we give the conventional perturbative treatment and demonstrate the thermodynamic inconsistency in its naive extension to lower densities. Then in Sec. III, we determine a chemical-potential dependent baglike coupling constant which makes the thermodynamic treatment self-consistent. After that we study, respectively, the properties of SQM and the structure of compact stars with the new EPQ model in Secs. IV and V. Finally Sec. VI is a short summary.

II. THE CONVENTIONAL PERTURBATION MODEL AND INCONSISTENCY OF ITS NAIVE EXTRAPOLATION

Let us start our paper from the perturbative expansion of the thermodynamic potential density of cold quark matter with two-flavor massless light quarks plus one massive strange quark. According to Eqs. (1) and (2) in Refs. [51,52], we have the perturbative contribution to the thermodynamic potential density as

$$\Omega^{\text{pt}} = \Omega_u + \Omega_d + \Omega_s, \quad (1)$$

where, to the first order, the contributions from massless up and down quarks are respectively

$$\Omega_u = -\frac{\mu_u^4}{4\pi^2}(1-2\alpha) \quad \text{and} \quad \Omega_d = -\frac{\mu_d^4}{4\pi^2}(1-2\alpha), \quad (2)$$

and that from the massive strange quarks is [51,53]

$$\begin{aligned} \Omega_s = & \frac{-1}{4\pi^2} \left[\mu_s \nu_s \left(\mu_s^2 - \frac{5}{2} m_s^2 \right) + \frac{3}{2} m_s^4 \text{ach} \frac{\mu_s}{m_s} \right] \\ & + \frac{\alpha}{2\pi^2} \left[3 \left(\mu_s \nu_s - m_s^2 \text{ach} \frac{\mu_s}{m_s} \right)^2 - 2\nu_s^4 \right. \\ & \left. + m_s^2 \left(6 \ln \frac{u}{m_s} + 4 \right) \left(\mu_s \nu_s - m_s^2 \text{ach} \frac{\mu_s}{m_s} \right) \right]. \quad (3) \end{aligned}$$

Here μ_u , μ_d , and μ_s are the chemical potentials of up, down, and strange quarks respectively, u is the renormalization

subtraction point, $\alpha \equiv \alpha_s/\pi = g^2/(4\pi^2)$ is the running coupling, and $\text{ach}x \equiv \ln(x + \sqrt{x^2 - 1})$ is the inverse hyperbolic cosine function. Because the mass of u and d quarks is much smaller than that of s quarks, we consider only the mass effect of strange quarks. For simplicity, we have used the notation $\nu_s \equiv \sqrt{\mu_s^2 - m_s^2}$, which can be regarded as the fermion momentum of s quarks. Because the electron does not participate in the strong interactions, its contribution to the thermodynamic potential is then

$$\Omega_e = -\frac{\mu_e^4}{12\pi^2}. \quad (4)$$

The number densities of u and d quarks and electrons are, respectively

$$n_u = \frac{\mu_u^3}{\pi^2}(1-2\alpha), \quad n_d = \frac{\mu_d^3}{\pi^2}(1-2\alpha), \quad n_e = \frac{\mu_e^3}{3\pi^2}, \quad (5)$$

while the density of s quarks is

$$n_s = \frac{\nu_s^3}{\pi^2} - \frac{2\alpha}{\pi^2} \nu_s \left(\mu_s \nu_s + 2m_s^2 - 3m_s^2 \ln \frac{\mu_s + \nu_s}{u} \right). \quad (6)$$

Here we should keep in mind that all terms with order in the coupling higher than unity have been discarded because we assume the perturbative expression is merely valid to leading order.

The thermodynamic potential density of the whole system composed of u, d, s quarks and electrons, given by the sum of Eqs. (2) to (4), depends explicitly on the chemical potentials μ_u , μ_d , μ_s , μ_e , and implicitly on the renormalization subtraction u via the coupling $\alpha(u)$ and the quark mass $m_s(u)$.

The running coupling $\alpha(u)$ and the running mass $m_s(u)$ of strange quarks are determined by the following renormalization group (RG) equations:

$$\frac{d\alpha}{d \ln u^2} = -\sum_{j=0}^{\mathcal{N}-1} \beta_j \alpha^{j+2} \equiv \beta(\alpha), \quad (7)$$

$$\frac{d \ln m_s}{d \ln u^2} = -\sum_{i=0}^{\mathcal{N}-1} \gamma_i \alpha^{i+1} \equiv \gamma(\alpha), \quad (8)$$

where \mathcal{N} is the loop number, while the beta and gamma functions, $\beta(\alpha)$ and $\gamma(\alpha)$, are presently known to four-loop level, given by the corresponding beta and gamma coefficients, i.e., β_i and γ_i . The original ones were given in the minimum subtraction scheme or its modified version ($\overline{\text{MS}}$). The coupling and masses given with these β_i and γ_i are, in principle, not continuous at heavy quark thresholds. In order to give a continuous coupling and a continuous

strange quark mass, the beta and gamma coefficients should be recombined. For the number of colors $N_c = 3$, these coefficients are provided in the Appendix. Comparing these coefficients with the original beta and gamma functions [60,61], one finds that $\beta_0, \beta_1, \gamma_0$, and γ_1 are not changed and thus universal [62], while modifications are necessary for $\beta_{j \geq 2}$ and $\gamma_{j \geq 2}$.

The exact solutions of Eqs. (7) and (8) can be obtained by separation of variables, as shown in the Appendix. At one-loop level, the running coupling and running quark mass of strange quarks are, respectively, given by

$$\alpha(u) = \frac{1}{\beta_0 \ln(u^2/\Lambda^2)}, \quad m_s = \hat{m}_s \alpha^{\gamma_0/\beta_0}, \quad (9)$$

where $\beta_0 = 11/4 - N_f/6$, $\gamma_0 = 1$, Λ and \hat{m}_s are the QCD scale parameters respectively for the coupling and strange quark mass.

With the requirement of continuity at the threshold of heavy quark masses and the initial condition $\alpha_s(M_Z) = 0.1185$ (where $M_Z = 91.1876$ MeV is the mass of Z bosons) and $m_s(2 \text{ GeV}) = 93.5$ MeV [63], one can get distinct coupling scale Λ_{N_f} and mass scale \hat{m}_{s,N_f} for a different effective number of flavors, i.e., Λ_{3-6} and $\hat{m}_{s,3-6}$, respectively corresponding to u in a different range, i.e., $u < m_c$, $m_c < u < m_b$, $m_b < u < m_t$, $u > m_t$, where $m_c = 1.275$ GeV, $m_b = 4.18$ GeV, $m_t = 173.21$ GeV [63]. The results to four-loop level and for a different number of flavors are given in Table I. Because we are considering three flavors to the leading order, in the following calculations we take $\Lambda = \Lambda_3 = 146$ MeV and $\hat{m}_s = \hat{m}_{s,3} = 280$ MeV, respectively.

Now we need to choose the relation between the renormalization point u and the chemical potentials. In principle, the choice is not unique. In Ref. [51], it is chosen to be

$$u = \frac{2}{3}(\mu_u + \mu_d + \mu_s). \quad (10)$$

To maintain weak equilibrium, the chemical potentials satisfy

$$\mu_u + \mu_e = \mu_d = \mu_s. \quad (11)$$

Furthermore, SQM should be in the state of charge neutrality, i.e.,

$$\frac{2}{3}n_u - \frac{1}{3}n_d - \frac{1}{3}n_s - n_e = 0. \quad (12)$$

Another condition for the quark system is the baryon number conservation, reading

$$n_b = \frac{1}{3}(n_u + n_d + n_s). \quad (13)$$

For a given baryon number density n_b we can solve Eqs. (11)–(13) to obtain all the relevant chemical potentials. Then the pressure P and the energy density E are given by

$$P = -\Omega, \quad (14)$$

$$E = \Omega + \sum_i \mu_i n_i, \quad (15)$$

where i goes over all flavors and electron.

To check thermodynamic consistency of phenomenological models, a discriminant Δ , as a function of the baryon number density, was introduced in Ref. [41] as

$$\begin{aligned} \Delta &= P - n_b^2 \frac{d}{dn_b} \left(\frac{E}{n_b} \right) \\ &= P + E - n_b \frac{dE}{dn_b}, \end{aligned} \quad (16)$$

where E and P are respectively model-given energy density and pressure. For any thermodynamically consistent models, the discriminant vanishes at arbitrary density.

In order to show the inconsistency degree of the above described pure perturbation model, we show in Fig. 1 the density behavior of the ratio Δ/E as a function of the density n_b . From this figure, one can easily find that the discriminant ratio decreases monotonically with increasing density. This is a clear demonstration that the thermodynamics at higher density is nearly consistent while the thermodynamic inconsistency becomes more and more serious with decreasing density.

One might think that this problem can be solved by adding a pure constant B_0 to the energy density (subtracting from the pressure) and interpreting it as the vacuum energy density, just like what had been done in the original bag model. In Fig. 2, we plot the energy per baryon (left axis) and pressure (right axis) as a function of the density for $\sqrt[4]{B_0} = 135$ MeV. It is obvious in this case that there exists

TABLE I. The QCD scale parameters Λ_{N_f} and \hat{m}_{s,N_f} in MeV to four-loop level for the number of flavors N_f from 3 to 6.

| Loop number | Λ_3 | Λ_4 | Λ_5 | Λ_6 | $m_{s,3}$ | $m_{s,4}$ | $m_{s,5}$ | $m_{s,6}$ |
|-------------|-------------|-------------|-------------|-------------|-----------|-----------|-----------|-----------|
| 1 | 146.2 | 122.9 | 90.44 | 44.03 | 279.9 | 303.5 | 339.5 | 401.4 |
| 2 | 365.3 | 309.5 | 217.9 | 90.65 | 248.2 | 263.8 | 291.0 | 341.4 |
| 3 | 342.4 | 297.1 | 213.4 | 89.93 | 242.5 | 257.0 | 283.4 | 332.4 |
| 4 | 339.1 | 295.7 | 212.7 | 89.67 | 240.3 | 254.3 | 280.4 | 329.0 |

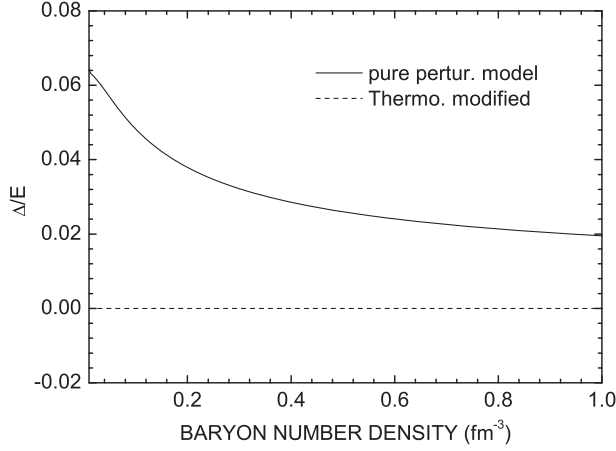


FIG. 1. The discriminant ratio Δ/E as a function of density. The solid curve is from the pure perturbation model, while the near horizontal line is from the EPQ model in the present paper.

a minimum energy per baryon (marked with a solid triangle) and zero pressure (the small open circle). As emphasized in Ref. [38], also directly seen from the first equality of Eq. (16), these two points should appear exactly at the same density. However, Fig. 2 clearly shows that they obviously deviate from each, contradicting the fundamental thermodynamics. This is understandable from the second equality of Eq. (16): adding a constant to E and subtracting it simultaneously from the pressure P does not influence the value of the discriminant Δ . In fact, if one draws the density behavior of Δ , one will find that it is totally overlapped with the case without the constant.

In the following section we will find an additional term that depends on chemical potentials. The chemical-potential-dependent term can be neglected at high density but it takes an important role at lower density, solving the thermodynamic inconsistency very nicely. The key point is that the renormalization subtraction u as a function of

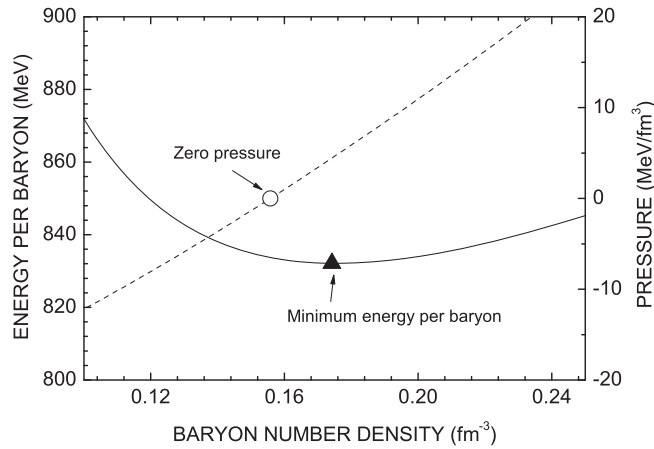


FIG. 2. Density behavior of the energy per baryon in pQCD with a running coupling in Eq. (10) and a bag constant of $B_0 = (135 \text{ MeV})^4$.

the chemical potentials cannot be arbitrarily taken, such as that in Eq. (10). Instead, we choose it to satisfy an equation obtained by the requirement of thermodynamic consistency.

III. EXTRAPOLATION WITH THERMODYNAMIC CONSISTENCY

The thermodynamic potential density of a cold quark system from perturbative QCD to order N can be generally written as

$$\Omega_N^{\text{pt}} = \sum_{i=0}^N \omega_i(\mu_u, \mu_d, \mu_s, m_s, \ln \alpha, u) \alpha^i, \quad (17)$$

where $\alpha = \alpha_s/\pi = g^2/(4\pi^2)$ is the QCD running coupling, m_s is the running mass of a strange quark. They satisfy the renormalization group equation given in Eqs. (7) and (8).

The corresponding number density for quark flavor $q = u, d, s$ can be easily obtained by the normal thermodynamic relation $n_q = -d\Omega^{\text{pt}}/d\mu_q$. Also at the order N , it gives

$$n_q = \sum_{k=0}^N \left[-\frac{\partial \omega_k}{\partial \mu_q} - \frac{\partial \omega_k}{\partial u} \frac{\partial u}{\partial \mu_q} + \frac{2}{u} \frac{\partial u}{\partial \mu_q} \sum_{i=0}^{k-1} f_{i,k-i-1} \right] \alpha^k, \quad (18)$$

where $f_{i,j}$ ($j = k - i - 1$) is zero if $i < 0$ or $j < 0$, otherwise it is defined to be

$$f_{i,j} = \left(i\omega_i + \frac{\partial \omega_i}{\partial \ln \alpha} \right) \beta_j + m_s \frac{\partial \omega_i}{\partial m_s} \gamma_j. \quad (19)$$

We write the whole thermodynamic potential density of the system as

$$\Omega = \Omega_N^{\text{pt}} + \Omega'. \quad (20)$$

Here Ω_N^{pt} is the perturbative contribution, while Ω' is the nonperturbative contribution. To determine Ω' , we require that it makes Ω satisfy the fundamental thermodynamic equation

$$d\Omega = -SdT - \sum_i n_i d\mu_i, \quad (21)$$

where S is the entropy density at temperature T . At zero temperature the first term vanishes and we have $d\Omega = -\sum_i n_i d\mu_i$. Substituting Eqs. (20), (17), and (18) into this equality, we immediately obtain

$$d\Omega' = \frac{\partial \Omega'}{\partial \mu_u} d\mu_u + \frac{\partial \Omega'}{\partial \mu_d} d\mu_d + \frac{\partial \Omega'}{\partial \mu_s} d\mu_s, \quad (22)$$

where the partial derivatives are

$$\frac{\partial \Omega'}{\partial \mu_u} = \frac{2}{u} \frac{\partial u}{\partial \mu_u} \sum_{k,i}^{(N,\mathcal{N})} f_{i,k-i-1} \alpha^k \equiv G_1(\mu_u, \mu_d, \mu_s), \quad (23)$$

$$\frac{\partial \Omega'}{\partial \mu_d} = \frac{2}{u} \frac{\partial u}{\partial \mu_d} \sum_{k,i}^{(N,\mathcal{N})} f_{i,k-i-1} \alpha^k \equiv G_2(\mu_u, \mu_d, \mu_s), \quad (24)$$

$$\frac{\partial \Omega'}{\partial \mu_s} = \frac{2}{u} \frac{\partial u}{\partial \mu_s} \sum_{k,i}^{(N,\mathcal{N})} f_{i,k-i-1} \alpha^k \equiv G_3(\mu_u, \mu_d, \mu_s). \quad (25)$$

The double summation in Eqs. (23)–(25) is given by

$$\sum_{k,i}^{(N,\mathcal{N})} \equiv \sum_{k=N+1}^{N+\mathcal{N}} \sum_{i=\max(0,k-N)}^{\min(k-1,N)}. \quad (26)$$

Therefore, the additional term Ω' is given by a path integral as

$$\Omega' = \int_{\mu_0}^{\mu} (G_1 d\mu_u + G_2 d\mu_d + G_3 d\mu_s) + B_0, \quad (27)$$

where $\mu_0 = (\mu_{u0}, \mu_{d0}, \mu_{s0})$ is a starting point for the path integral which is fixed to be $\mu_{u0} = \mu_{d0} = \mu_{s0} = 313$ MeV in the present calculation, while its moving effect is boiled down to another constant B_0 .

As everyone knows, the thermodynamic potential is a state function. Therefore, Ω' should be independent of the path, namely, the integration in Eq. (27) is path independent. This requires that the integrands satisfy the Cauchy conditions

$$\frac{\partial G_1}{\partial \mu_d} = \frac{\partial G_2}{\partial \mu_u}, \quad \frac{\partial G_2}{\partial \mu_s} = \frac{\partial G_3}{\partial \mu_d}, \quad \frac{\partial G_1}{\partial \mu_s} = \frac{\partial G_3}{\partial \mu_u}. \quad (28)$$

It is easy to prove that only two of them are independent.

In the present paper, let us take the first order of Ω_N^{pt} as an example, i.e., Ω_1^{pt} , with running coupling α and running mass m_s expanded to first order which are explicitly given by Eq. (9). In this case, we have

$$G_1 = \frac{2}{u} \frac{\partial u}{\partial \mu_u} f_{1,0} \alpha^2, \quad G_2 = \frac{2}{u} \frac{\partial u}{\partial \mu_d} f_{1,0} \alpha^2, \quad (29)$$

$$G_3 = \frac{2}{u} \frac{\partial u}{\partial \mu_s} f_{1,0} \alpha^2.$$

With the notation $\tau \equiv \sqrt[4]{\mu_u^4 + \mu_d^4 + \mu_s^4}$ and the expressions of ω_0 and ω_1 , i.e.,

$$\omega_0 = \frac{-1}{4\pi^2} \left[\tau^4 + \mu_s \nu_s \left(\mu_s^2 - \frac{5}{2} m_s^2 \right) + \frac{3}{2} m_s^4 \text{ach} \frac{\mu_s}{m_s} \right],$$

$$\omega_1 = \frac{1}{2\pi^2} \left[\tau^4 - 2\nu_s^4 + 3 \left(\mu_s \nu_s - m_s^2 \text{ach} \frac{\mu_s}{m_s} \right)^2 + m_s^2 \left(6 \ln \frac{u}{m_s} + 4 \right) \left(\mu_s \nu_s - m_s^2 \text{ach} \frac{\mu_s}{m_s} \right) \right], \quad (30)$$

one can derive the explicit expression of $f_{1,0}$, giving

$$f_{1,0} = \beta_0 \omega_1 + \gamma_0 m_s \frac{\partial \omega_1}{\partial m_s}$$

$$= \frac{9}{8\pi^2} (\mu_u^4 + \mu_d^4 + \mu_s^4) + \frac{75 m_s^4}{8\pi^2} \text{ach}^2 \left(\frac{\mu_s}{m_s} \right)$$

$$+ \frac{m_s^2}{8\pi^2} \left[41 \mu_s^2 - 50 m_s^2 + 44 \mu_s \nu_s \right.$$

$$+ 6 \ln \frac{u}{m_s} \left(17 \mu_s \nu_s - 25 m_s^2 \text{ach} \frac{\mu_s}{m_s} \right)$$

$$\left. - 2 \text{ach} \frac{\mu_s}{m_s} (38 m_s^2 + 51 \mu_s \nu_s) \right]. \quad (31)$$

Substituting Eq. (29) into the first two Cauchy conditions, we have

$$\frac{\partial u}{\partial \mu_u} \frac{\partial f_{1,0}}{\partial \mu_d} = \frac{\partial u}{\partial \mu_d} \frac{\partial f_{1,0}}{\partial \mu_u}, \quad \frac{\partial u}{\partial \mu_d} \frac{\partial f_{1,0}}{\partial \mu_s} = \frac{\partial u}{\partial \mu_s} \frac{\partial f_{1,0}}{\partial \mu_d}. \quad (32)$$

From Eq. (31), one can get the partial derivatives of $f_{1,0}$ with respect to μ_u and μ_d respectively, i.e.,

$$\frac{\partial f_{1,0}}{\partial \mu_u} = \frac{9 \mu_u^3}{2\pi^2}, \quad \frac{\partial f_{1,0}}{\partial \mu_d} = \frac{9 \mu_d^3}{2\pi^2}. \quad (33)$$

Using Eq. (33), the first equation in Eq. (32) becomes

$$\mu_u^3 \frac{\partial u}{\partial \mu_d} = \mu_d^3 \frac{\partial u}{\partial \mu_u}. \quad (34)$$

This equation means that the solution of u is a function of μ_s and $\rho \equiv \sqrt[4]{\mu_u^4 + \mu_d^4}$, i.e., $u = u(\rho, \mu_s)$. However, this function is not necessarily explicit, and can be generally implicit. So we assume it is determined by the following implicit equation:

$$\Phi(\rho, \mu_s, u) = 0. \quad (35)$$

In order to find the form of Φ , we give the partial derivatives of u with respect to μ_d and μ_s , i.e.,

$$\frac{\partial u}{\partial \mu_d} = \frac{\partial u}{\partial \rho} \frac{\partial \rho}{\partial \mu_d} = -\frac{\Phi_\rho}{\Phi_u} \frac{\partial \rho}{\partial \mu_d}, \quad \frac{\partial u}{\partial \mu_s} = -\frac{\Phi_{\mu_s}}{\Phi_u}, \quad (36)$$

where the notations $\Phi_x \equiv \partial\Phi/\partial x$ ($x = \rho, u, \mu_s$) have been used. Then substituting Eq. (36) to the second equation in Eq. (32) leads to

$$\frac{8\pi^2}{9} \frac{\partial f_{1,0}}{\partial \mu_s} \frac{\partial \Phi}{\partial \rho} = 4\rho^3 \frac{\partial \Phi}{\partial \mu_s}, \quad (37)$$

where $\frac{\partial f_{1,0}}{\partial \mu_s}$ can be obtained from Eq. (31), i.e.,

$$\begin{aligned} \frac{\partial f_{1,0}}{\partial \mu_s} &= \frac{m_s^2}{2\pi^2 \nu_s^2} [\nu_s(22\mu_s^2 - 30m_s^2) + \mu_s(5m_s^2 - 14\mu_s^2)] \\ &+ \frac{9\mu_s^5}{2\pi^2 \nu_s^2} - \frac{3m_s^2}{2\pi^2 \nu_s} (17\mu_s^2 - 21m_s^2) \ln \frac{\mu_s + \nu_s}{u}. \end{aligned} \quad (38)$$

For Eq. (37) to be fulfilled, we choose

$$\frac{\partial \Phi}{\partial \rho} = 4\rho^3, \quad \frac{\partial \Phi}{\partial \mu_s} = \frac{8\pi^2}{9} \frac{\partial f_{1,0}}{\partial \mu_s}. \quad (39)$$

Solving the equalities in Eq. (39), we can find the solution

$$\Phi = \frac{8\pi^2}{9} f_{1,0} - \phi(u), \quad (40)$$

where $\phi(u)$ is an arbitrary function of u . In fact, integrating the first equality in Eq. (39), one can get the solution as $\Phi(\rho, \mu_s, u) = \rho^4 + \varphi(\mu_s, u)$, where the integration constant φ (with respect to the variables μ_s and u) can be obtained by substituting into the second equality of Eq. (39) as

$$\varphi(\mu_s, u) = \frac{8\pi^2}{9} \int \frac{\partial f_{1,0}}{\partial \mu_s} d\mu_s - \rho^4 - \phi(u),$$

which gives the solution in Eq. (40) immediately.

For convenience and simplicity, we have chosen the function $\phi(u) = N_f(u/C)^4$ with constant C being a model parameter which can be fixed in a reasonable region by the common knowledge of modern nuclear physics. So, from the solution of Eq. (32), one can find that to solve the problem of inconsistency in thermodynamics, the relation between the renormalization subtraction point u and chemical potentials should be obtained by solving the following equation:

$$\frac{8\pi^2}{9} f_{1,0}(\rho, \mu_s, u) - \frac{N_f}{C^4} u^4 = 0. \quad (41)$$

As is well known, the mass effect from strange quarks can be ignored at very high density. In this case the relation between the renormalization subtraction point and chemical potentials can be given in a simple form, i.e.,

$$u = C \sqrt[4]{\frac{\mu_u^4 + \mu_d^4 + \mu_s^4}{N_f}}, \quad (42)$$

which can be obtained by taking $m_s \rightarrow 0$ in Eq. (41).

In order to get the EOS, in general one should numerically solve Eq. (41). Then substituting Eq. (29) to Eq. (27) and numerically integrating it, one can get the quantity Ω' which is essential in fixing the problem of thermodynamic inconsistency. The partial derivatives of renormalization subtraction point u with respect to chemical potentials μ_q ($q = u, d, s$) in Eq. (29) are

$$\frac{\partial u}{\partial \mu_q} = \frac{\partial f_{1,0}/\partial \mu_q}{\frac{9N_f u^3}{2\pi^2 C^4} - \frac{\partial f_{1,0}}{\partial u} - \frac{\partial f_{1,0}}{\partial m_s} \frac{\partial m_s}{\partial \alpha} \frac{\partial \alpha}{\partial u}}, \quad (43)$$

where $\partial f_{1,0}/\partial \mu_q$ are already given in Eqs. (33) and (38). Other relevant derivatives of $f_{1,0}$ in Eq. (43) are, respectively

$$\frac{\partial f_{1,0}}{\partial u} = \frac{3m_s^2}{4\pi^2 u} \left(17\mu_s \nu_s - 25m_s^2 \text{ach} \frac{\mu_s}{m_s} \right) \quad (44)$$

and

$$\begin{aligned} \frac{\partial f_{1,0}}{\partial m_s} &= \frac{75}{2\pi^2} m^3 \text{ach}^2 \left(\frac{\mu_s}{m_s} \right) - \left[\frac{75}{\pi^2} m_s^3 \ln \frac{u}{m_s} \right. \\ &+ \left. \frac{m_s}{4\pi^2 \nu_s} (78\mu_s \nu_s^2 + 77m_s^2 \nu_s + 24\mu_s^3) \right] \\ &\times \text{ach} \frac{\mu_s}{m_s} - \frac{3m_s \mu_s}{2\pi^2 \nu_s} (13m_s^2 - 17\mu_s^2) \\ &\times \ln \frac{u}{m_s} + \frac{m_s}{4\pi^2 \nu_s^2} (23m_s^2 \mu_s \nu_s + 92\mu_s^4 + 100m_s^4 \\ &- 7\mu_s^3 \nu_s - 192m_s^2 \mu_s^2). \end{aligned} \quad (45)$$

The remaining derivatives on the right-hand side of Eq. (43) are

$$\frac{\partial m_s}{\partial \alpha} = \frac{4\hat{m}_s}{9} \alpha^{-\frac{5}{9}} \quad \text{and} \quad \frac{\partial \alpha}{\partial u} = -\frac{9\alpha^2}{2u}. \quad (46)$$

IV. EOS OF STRANGE QUARK MATTER

As is usually done, we assume SQM to be a mixture of interacting quarks and free electrons. So the total thermodynamic potential density Ω_{tot} reads

$$\Omega_{\text{tot}} = \Omega^{\text{pt}} - \frac{\mu_e^4}{12\pi^2} + \Omega', \quad (47)$$

where the first term is the perturbative contribution in Eq. (17) whose concrete form is given to leading order in Eqs. (2) and (3). The second term is the contribution from electrons treated as free particles because they do not

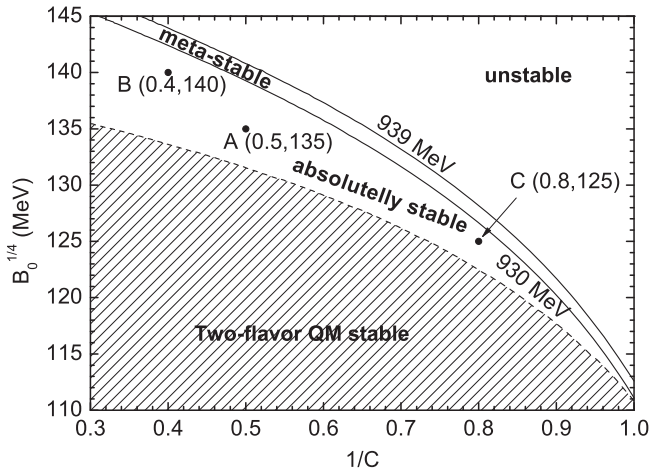


FIG. 3. The parameter range in $B_0^{1/4}$ vs $1/C$ plane. The shaded region is forbidden where two-flavor quark matter is stable. The energy per baryon of three-flavor quark matter is bigger than 939 MeV in the right upper region marked with “unstable,” less than 939 MeV but bigger than 930 MeV in the region with “metastable,” smaller than 930 MeV in the absolutely stable region where three sets of parameters A, B, and C are indicated by solid dots.

participate in the strong interactions, and the last term is given in Eq. (27), determined by thermodynamic consistency requirement to consider the nonperturbative effect.

For a given baryon number density, one can solve Eqs. (11)–(13) with the help of Eqs. (5) and (6) to obtain the relevant particle chemical potentials, then all other quantities can be thermodynamically obtained. But in the present model, there are still two parameters, B_0 and C , to be determined by stability arguments.

As is well known, the energy per baryon of two-flavor quark matter should be bigger than 930 MeV ($E/n_b > 930$ MeV), in order not to contradict standard nuclear physics. Therefore, the shaded region in Fig. 3 is forbidden. If the energy per baryon of three flavor quark matter is less than 930 MeV, the SQM is absolutely stable; if it is bigger than 930 MeV, but smaller than 939 MeV, the SQM is metastable; otherwise, the SQM is unstable. These different regions are indicated in Fig. 3.

To investigate the properties of SQM in the present EPQ model, we choose three typical sets of parameters in the absolutely stable region, i.e., $(1/C, \sqrt[4]{B_0}/\text{MeV}) = (0.5, 135), (0.4, 140), (0.8, 125)$, respectively represented with capital letters A, B, and C in Fig. 3.

Let us first check the consistency of EPQ model. Figure 4 shows the density behavior of the energy per baryon with different parameters. It is obvious that the minimum energy per baryon for each curve locates exactly at the density corresponding to zero pressure. This consistency in thermodynamics can be seen in Fig. 1 where the value of Δ/E for the present model is zero at all densities. In addition, the three minimum points in this figure

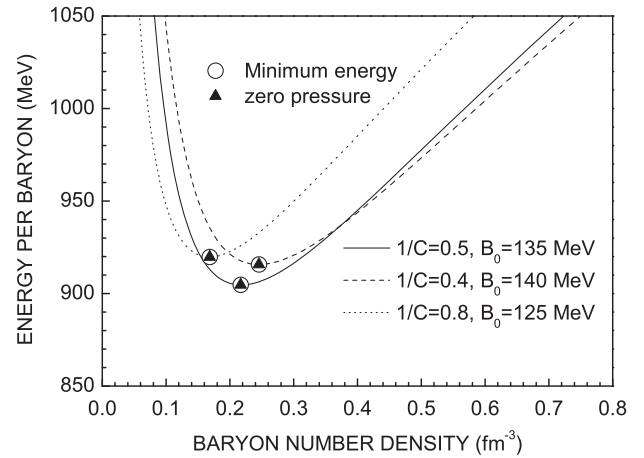


FIG. 4. Density behavior of the energy per baryon. It is obvious that the minimum energy (the triangle) for each curve locates exactly at the density corresponding to zero pressure (the circle).

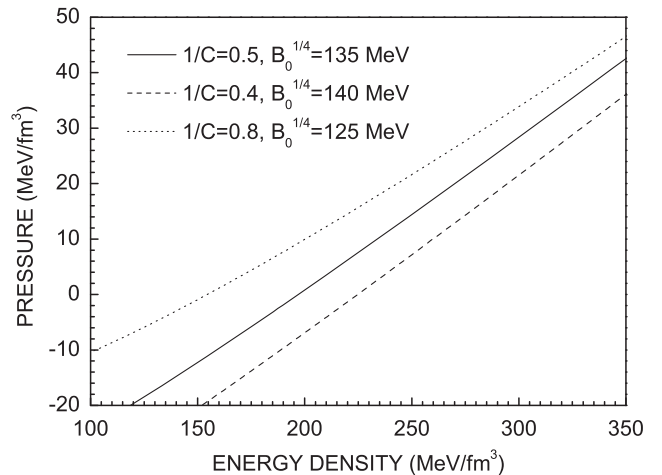


FIG. 5. The EOS of SQM for the three typical parameter sets.

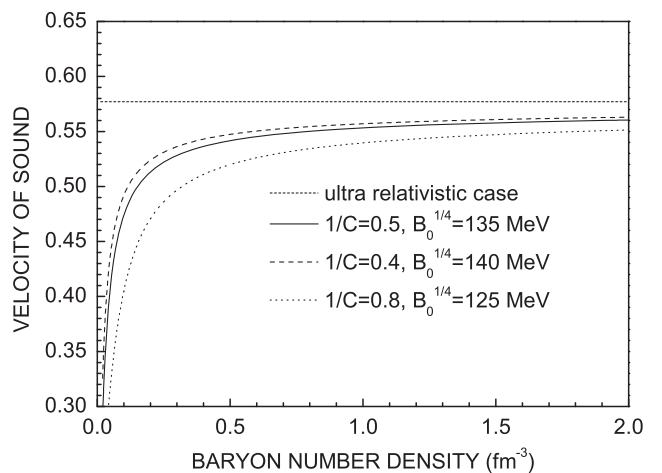
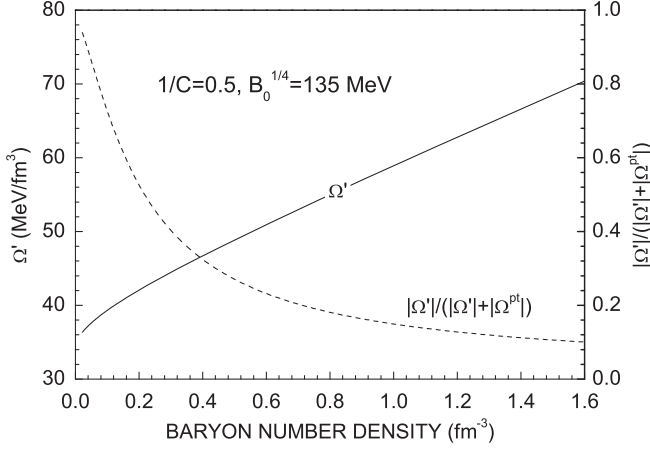


FIG. 6. Velocity of sound in SQM. The nearly horizontal line is for the ultrarelativistic case, the three lower curves are from the present model for the three typical sets of parameters.

FIG. 7. The density behavior of Ω' and its relative importance.

correspond to absolutely stable SQM, as expected. It is also found that the minimum energy per baryon in fact becomes bigger with decreasing C and/or increasing B_0 .

Figure 5 gives the EOS of SQM. The stiffness of EOS obviously varies with the model parameters C and B_0 , e.g., EOS would become stiffer with bigger C and/or smaller B_0 . In the next section we will see that this means a bigger maximum mass of compact stars (see Fig. 8).

To check the impact of the additional term Ω' , we plot in Fig. 6 the density behavior of the velocity of sound calculated by

$$v = \sqrt{\left| \frac{dP}{dE} \right|}. \quad (48)$$

We have noted that the density behavior of sound velocity is greatly affected by the stiffness of EOS, and it is understandable that stiffer EOS corresponds to fast velocity of sound. At very high density, however, they all approach to the ultrarelativistic case. In addition, we would like to point out that the sound velocity is independent of the parameter B_0 .

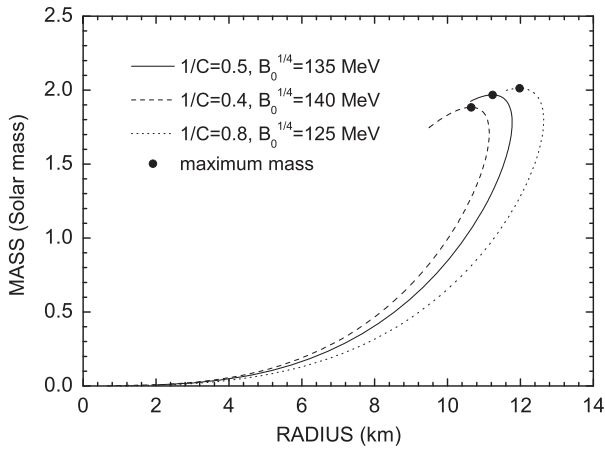


FIG. 8. The mass-radius relation of quark stars.

Figure 7 shows the density behavior of Ω' and its relative importance. From this figure one can see that, although Ω' increases with increasing density, the relative importance decreases with increasing density. That means Ω' plays a relatively important role at lower density while it is ignorable at high density. In this regard it is similar to a chemical-potential-dependent bag constant.

V. STRUCTURE OF STRANGE STARS

Neutron stars are the main targets of future observatories [64–67] and have long been interesting objects of many theoretical and observational investigations [3,48,49,68–71]. Because their inner matter is very dense, they become the most promising places to find quark matter [72,73].

In the general case, such a compact object may be a hybrid star with pure quark core and hadronic crust [8]. Because SQM can be self-bound, i.e., its internal pressure can be zero at a definite density (see the minima in Fig. 4), the whole star can be converted to a pure quark star, for example, as a strong deflagration process during a few milliseconds [74], or seeded with slets [75] by the self-annihilating weakly interacting massive particles [76], etc.

In the preceding sections, we have developed an enhanced version of a perturbative QCD treatment of the dense quark matter by thermodynamic consistency requirement. Now we apply it to study the structure of quark stars. For this purpose we should solve the Tolman-Oppenheimer-Volkov equation [77]

$$\frac{dP}{dr} = -\frac{GmE(1+P/E)(1+4\pi r^3 P/m)}{r^2(1-2Gm/r)}, \quad (49)$$

with the subsidiary condition

$$\frac{dm}{dr} = 4\pi r^2 E, \quad (50)$$

where $G = 6.707 \times 10^{-45} \text{ MeV}^{-2}$ is the gravitational constant, r is the distance from the center of a quark star, and P and E are the pressure and energy density with their mutual relation given by EOS. One can refer to Ref. [38] for a concise process of how to solve this equation.

On application of the equations of state in Fig. 5, we can get the mass-radius relation in Fig. 8 for the typical parameter sets indicated in the legend. This figure shows several features of quark stars. (1) The radius of a quark star can be in principle very small, i.e., there is no lower bound to the radius. This is very different from the normal neutron stars whose radii are normally greater than a critical value. (2) For a given set of parameters, the star radius first increases with increasing the star mass, until a maximum radius is reached. After that, the radius decreases until the maximum star mass is arrived. (3) The maximum star mass depends on parameters. It actually increases with increasing C , while it decreases with increasing B_0 . Especially for

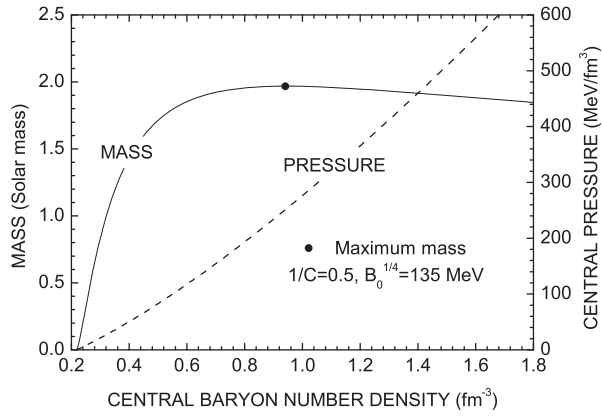


FIG. 9. The mass and central pressure of the quark star as functions of the central density for the typical parameters $1/C = 0.5$ (or $C = 2$) and $B_0^{1/4} = 135$ MeV.

the typical parameters $C = 2$ and $B_0 = (135 \text{ MeV})^4$, the maximum mass is about 2 times the solar mass, consistent with the recent high-mass observations [69,70].

To understand the existence of a maximum star mass, we show, in Fig. 9 for the parameter set A, the star mass as a function of the central density, with the central pressure also given on the right axis. One can easily find that the star mass first increases with increasing the central density to a

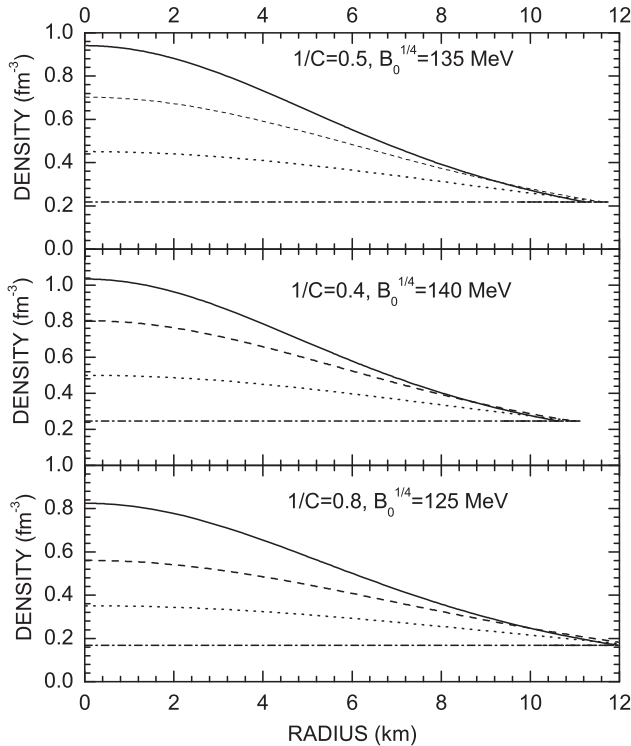


FIG. 10. Density profiles for different sets of parameters indicated in the legends. The solid curve in each panel is for the highest central density corresponding to the quark star with maximum mass, while the horizontal represents the surface density.

TABLE II. Characteristic quantities for the typical parameter sets $(C^{-1}, B_0^{1/4}/\text{MeV}) = (0.5, 135)$, $(0.4, 140)$, and $(0.8, 125)$. The second through sixth rows give, respectively, the maximum mass M_{max} , the radius corresponding to the maximum mass $R(M_{\text{max}})$, the highest central density at the maximum mass n_{max} , the surface density n_0 and the corresponding energy per baryon E_0/n_0 .

| $(1/C, B_0^{1/4}/\text{MeV})$ | (0.5,135) | (0.4,140) | (0.8,125) |
|---------------------------------------|-----------|-----------|-----------|
| M_{max}/M_{\odot} | 1.968 | 1.884 | 2.013 |
| $R(M_{\text{max}})$ [km] | 11.2 | 10.6 | 12.0 |
| n_{max} [fm^{-3}] | 0.941 | 1.034 | 0.8250 |
| n_0 [fm^{-3}] | 0.2177 | 0.2457 | 0.1683 |
| E_0/n_0 [MeV] | 904.7 | 915.7 | 919.8 |

critical density n_{max} . After this density, the star mass decreases with increasing the central density, and the star itself becomes mechanically unstable. The central pressure is always an increasing function of the central density. It approaches to zero if the quark star mass becomes zero. Please note, the corresponding central density to zero pressure is nonzero. Instead, it is a definite value corresponding to the surface density of the quark star.

The density of a quark star is not uniformly distributed. In Fig. 10, we plot the density profiles with different panels for different parameters. For each parameter set, the utmost curve corresponds to the star with the maximum mass, $r = 0$ corresponds to the central density. At the star surface, the pressure is zero. This point corresponds to the minimum energy per baryon in Fig. 4. Therefore, the surface density of the quark star is not zero, i.e., the star has a sharp surface. In Table II, we list some characteristic quantities of quark stars for each parameter set, including the maximum star mass to the solar mass M_{max}/M_{\odot} , the corresponding radius $R(M_{\text{max}})$, the highest central density n_{max} , the surface density n_0 , and the minimum energy per baryon E_0/n_0 .

It should be noted that the observation of quark stars having a sharp surface depends very much on the model assumption. Especially when one does not have a color-flavor locked phase throughout, the star might have a crust of ordinary matter supported by electrons extending beyond the quark surface, or the outer layers of the quark star might fragment to strangelets, somewhat similar to a normal neutron star crust. Also, for some parameters, e.g., the case C, the surface density is closer to the normal nuclear saturation density, which might be an indication of phase transition to nuclear matter. To understand possible phase transition in a mixed star, it is necessary to investigate the phase equilibrium condition in the phase boundary [8,40].

VI. SUMMARY

The perturbative QCD is important to study strongly interacting matter. However, its naive extension to

comparatively lower density has serious thermodynamic inconsistency problems due to the running of the QCD coupling and/or quark masses. We have tried to extend it by including an additional term in the thermodynamic potential density. The additional term is determined by the fundamental differential equation of thermodynamics. It takes an important role at comparatively lower density, but ignorable at high density, playing the role of a chemical-potential-dependent bag constant.

On application of the thermodynamically EPQ model, we study the properties of SQM and structure of quark stars. It is found that SQM still has the possibility of being absolutely stable in the present model, i.e., the minimum energy per baryon could be less than 930 MeV with zero internal pressure. This leads to the maximum mass of quark stars as large as 2 times the solar mass. The quark stars in the present model have several features, such as a sharp surface, no lower bound for the radius, the maximum mass of about 2 times the solar mass and a maximum radius of about 11 kilometers, etc.

Naturally, there are several aspects not included in the present investigations, e.g., the color superconductivity [32,78,79], a strong external magnetic field [58,80–82], etc. Furthermore, only zero temperature has been considered in the present paper. To investigate the properties of hot quark matter, such as the quark gluon plasma produced in high energy heavy ion collisions [83,84], the inclusion of finite temperature is of crucial importance. Therefore, more careful studies are necessary in the future.

ACKNOWLEDGMENTS

The authors would like to thank support from National Natural Science Foundation of China (No. 11135011, No. 11275125, No. 11221504, No. 11375070, and No. 11475110), Key Program at Chinese Academy of Sciences (No. KJCX3-SYW-N2), National Basic Research Program of China (No. 2015CB856904), Science and Technology Commission of Shanghai Municipality (No. 11DZ2260700), Program for Professor of Special Appointment (Eastern Scholar) at Shanghai Institutions of Higher Learning, and the “Shu Guang” project of Shanghai Municipal Education Commission and Shanghai Education Development Foundation.

APPENDIX: MATCHING-INVARIANT BETA AND GAMMA FUNCTIONS AND SOLUTIONS OF THE RENORMALIZATION EQUATIONS

A matching-invariant beta function was previously derived in Ref. [85]. The beta and gamma functions which give matching-invariant running coupling and running quark masses in QCD can be similarly obtained. In the present context, the beta and gamma coefficients are given by

$$\beta_i = \sum_{k=1}^{\min(1,i)} \beta_{i,k} N_f^k, \quad \gamma_i = \sum_{k=0}^i \gamma_{i,k} N_f^k, \quad (\text{A1})$$

where the color matrix elements, $\beta_{i,k}$ and $\gamma_{i,k}$, are independent of the number of flavors N_f , and for the number of colors $N_c = 3$, their values can be given, to the four-loop level, as

$$[\beta_{i,k}] = \begin{bmatrix} 11/4 & -1/6 & 0 & 0 \\ 51/8 & -19/24 & 0 & 0 \\ \frac{2857}{128} & -\frac{4549}{1152} & \frac{79}{1152} & 0 \\ 114.230 & -21.5548 & 1.01146 & \frac{23}{1152} \end{bmatrix} \quad (\text{A2})$$

and

$$[\gamma_{i,k}] = \begin{bmatrix} 1 & 0 & 0 & 0 \\ 101/24 & -5/36 & 0 & 0 \\ 1249/64 & -1.30380 & -31/324 & 0 \\ 98.9434 & -3.64007 & -0.78090 & \gamma_{3,3} \end{bmatrix}, \quad (\text{A3})$$

where $\gamma_{3,3} = \zeta_3/36 - 197/5832 \approx -0.00038868$.

In order to have full thermodynamic consistency in the present model, we need the exact solutions of the renormalization equation (7) at a given loop level. For this purpose, we can apply the approach of variable separation which gives

$$d \ln u^2 = \frac{d\alpha}{\beta(\alpha)} \equiv \left[\hat{\beta}(\alpha) + \frac{\beta_1}{\beta_0 \alpha} - \frac{1}{\alpha^2} \right] \frac{d\alpha}{\beta_0}, \quad (\text{A4})$$

where the acute beta function is defined to be $\hat{\beta}(\alpha) \equiv \beta_0/\beta(\alpha) - \beta_1/(\beta_0 \alpha) + 1/\alpha^2$. Using the expression of the beta function, one has

$$\hat{\beta}(\alpha) = \frac{\sum_{i=0}^{N-2} (\beta_{i+2} - \frac{\beta_1}{\beta_0} \beta_{i+1}) \alpha^i - \beta_N \alpha^{N-2}}{\sum_{i=0}^{N-1} \beta_i \alpha^i}. \quad (\text{A5})$$

Integrating both sides of Eq. (A4) gives

$$\ln \frac{u^2}{\Lambda^2} = \frac{1}{\beta_0 \alpha} + \frac{\beta_1}{\beta_0^2} \ln(\beta_0 \alpha) + \frac{1}{\beta_0^2} W_N(\alpha), \quad (\text{A6})$$

where the function $W_N(\alpha)$ is given by $W_N(\alpha) = \beta_0 \int_0^\alpha \hat{\beta}(x) dx$. For example, it is not difficult to give

$$W_2(\alpha) = -\beta_1 \ln \left(1 + \frac{\beta_1}{\beta_0} \alpha \right), \quad (\text{A7})$$

$$W_3(\alpha) = \frac{2\beta_0\beta_2 - \beta_1^2}{\sqrt{4\beta_0\beta_2 - \beta_1^2}} \arctan \frac{\sqrt{4\beta_0\beta_2 - \beta_1^2}}{\beta_1 + 2\beta_0/\alpha} - \frac{\beta_1}{2} \ln \left(\sum_{i=0}^2 \frac{\beta_i}{\beta_0} \alpha^i \right). \quad (\text{A8})$$

The Λ in Eq. (A6) is a QCD scale for the running coupling. In principle, it is an integration constant. The choice in Eq. (A6) is to be consistent with the conventional series expansion. For a chosen u , the corresponding α is obtained by numerically solving the algebraic equation (A6). At the one-loop level, the function $W_{\mathcal{N}}(\alpha)$ becomes $W_1(\alpha) = -\beta_1 \ln(\beta_0\alpha)$. In this case, an explicit solution can be easily obtained, as given in the first equality of Eq. (9).

To obtain the strange quark mass, we divide Eq. (8) by Eq. (7), giving

$$\frac{d \ln m_s}{d\alpha} = \frac{\gamma(\alpha)}{\beta(\alpha)} \equiv \frac{\gamma_0}{\beta_0\alpha} + I_{\mathcal{N}}(\alpha), \quad (\text{A9})$$

where the function $I_{\mathcal{N}}(\alpha)$ is defined by

$$I_{\mathcal{N}}(\alpha) \equiv \frac{\gamma(\alpha)}{\beta(\alpha)} - \frac{\gamma_0}{\beta_0\alpha} = \frac{\sum_{i=0}^{\mathcal{N}-2} (\gamma_{i+1} - \frac{\gamma_0}{\beta_0} \beta_{i+1}) \alpha^i}{\sum_{i=0}^{\mathcal{N}-1} \beta_i \alpha^i}. \quad (\text{A10})$$

Integrating Eq. (A9) then leads to

$$m_s = \hat{m}_s \alpha^{\gamma_0/\beta_0} \exp \left(\int_0^\alpha I_{\mathcal{N}}(x) dx \right), \quad (\text{A11})$$

where \hat{m}_s is a QCD mass scale of strange quarks. The definite integration in Eq. (A11), i.e., $\int_0^\alpha I_{\mathcal{N}}(x) dx \equiv w_{\mathcal{N}}(\alpha)$, can also be analytically carried out, e.g.,

$$w_2(\alpha) = \left(\frac{\gamma_1}{\beta_1} - \frac{\gamma_0}{\beta_0} \right) \ln \left(1 + \frac{\beta_1}{\beta_0} \alpha \right), \quad (\text{A12})$$

$$w_3(\alpha) = \frac{(\frac{\gamma_0}{\beta_0} - 2\frac{\gamma_1}{\beta_1} + \frac{\gamma_2}{\beta_2})}{\sqrt{4\beta_0\beta_2/\beta_1^2 - 1}} \arctan \frac{\sqrt{4\beta_0\beta_2/\beta_1^2 - 1}}{1 + 2\beta_0/(\beta_1\alpha)} + \frac{1}{2} \left(\frac{\gamma_2}{\beta_0} - \frac{\gamma_0}{\beta_0} \right) \ln \left(\sum_{i=0}^2 \frac{\beta_i}{\beta_0} \alpha^i \right). \quad (\text{A13})$$

Because $I_1(\alpha) = 0$, $w_1(\alpha)$ is also zero. Accordingly, Eq. (A11) leads to the second equality in Eq. (9) at the one-loop level.

-
- [1] *Proceedings of the 14th International Conference on Strangeness in Quark Matter (SQM 2013)*, Birmingham, UK, 2013, edited by D. Evans, S. Hands, R. Lietava, R. Romita, and O. V. Bailie [*J. Phys. Conf. Ser.* **509**, 011001 (2014)].
 - [2] A. Bodmer, *Phys. Rev. D* **4**, 1601 (1971).
 - [3] N. Itoh, *Prog. Theor. Phys.* **44**, 291 (1970).
 - [4] S. A. Chin and A. K. Kerman, *Phys. Rev. Lett.* **43**, 1292 (1979).
 - [5] H. Terazawa, Tokyo University Report No. INS-336, 1979.
 - [6] E. Witten, *Phys. Rev. D* **30**, 272 (1984).
 - [7] E. Farhi and R. L. Jaffe, *Phys. Rev. D* **30**, 2379 (1984).
 - [8] A. Li, W. Zuo, and G. X. Peng, *Phys. Rev. C* **91**, 035803 (2015).
 - [9] J. X. Hou, G. X. Peng, C. J. Xia, and J. F. Xu, *Chin. Phys. C* **39**, 015101 (2015).
 - [10] A. A. Isayev, *Phys. Rev. C* **91**, 015208 (2015).
 - [11] X. B. Zhang, Z. C. Bu, F. P. Peng, and Y. Zhang, *Nucl. Phys. A* **938**, 1 (2015).
 - [12] P. C. Chu and L. W. Chen, *Astrophys. J.* **780**, 135 (2014).
 - [13] P. C. Chu, L. W. Chen, and X. Wang, *Phys. Rev. D* **90**, 063013 (2014).
 - [14] L. Paulucci and J. E. Horvath, *Phys. Lett. B* **733**, 164 (2014).
 - [15] S. W. Chen, Q. Li, J. F. Xu, L. Gao, and C. J. Xia, *Int. J. Mod. Phys. E* **23**, 1450013 (2014).
 - [16] M. Sinha, X. G. Huang, and A. Sedrakian, *Phys. Rev. D* **88**, 025008 (2013).
 - [17] Q. Chang, S. W. Chen, G. X. Peng, and J. F. Xu, *Sci. China Phys. Mech. Astron.* **56**, 1730 (2013).
 - [18] S. W. Chen and G. X. Peng, *Commun. Theor. Phys.* **57**, 1037 (2012).
 - [19] H. H. Tang and G. X. Peng, *Commun. Theor. Phys.* **56**, 1071 (2011).
 - [20] H. Li, X. L. Luo, and H. S. Zong, *Phys. Rev. D* **82**, 065017 (2010).
 - [21] T. Bao, G. Z. Liu, E. G. Zhao, and M. F. Liu, *Eur. Phys. J. A* **38**, 287 (2008).
 - [22] C. Wu, W. L. Qian, and R. K. Su, *Phys. Rev. C* **77**, 015203 (2008).
 - [23] F. Karsch, *Lect. Notes Phys.* **583**, 209 (2002); S. Muroya, A. Nakamura, C. Nonaka, and T. Takaishi, *Prog. Theor. Phys.* **110**, 615 (2003).
 - [24] Y. Nambu and G. Jona-Lasino, *Phys. Rev.* **122**, 345 (1961); **124**, 246 (1961).
 - [25] T. Xia, L. Y. He, and P. F. Zhuang, *Phys. Rev. D* **88**, 056013 (2013).
 - [26] L. Chang, Y. X. Liu, and H. Guo, *Phys. Rev. D* **72**, 094032 (2005).
 - [27] V. Goloviznin and H. Satz, *Z. Phys. C* **57**, 671 (1993).
 - [28] A. Peshier, B. Kämpfer, O. P. Pavlenko, and G. Soff, *Phys. Lett. B* **337**, 235 (1994).

- [29] M. Bluhm, B. Kämpfer, and G. Soff, *Phys. Lett. B* **620**, 131 (2005).
- [30] V. M. Bannur, *Phys. Rev. C* **75**, 044905 (2007).
- [31] F. G. Gardim and F. M. Steffens, *Nucl. Phys. A* **825**, 222 (2009).
- [32] X. J. Wen, *Phys. Rev. D* **88**, 034031 (2013).
- [33] L. J. Luo, J. C. Yan, W. M. Sun, and H. S. Zong, *Eur. Phys. J. C* **73**, 2626 (2013).
- [34] G. N. Fowler, S. Raha, and R. M. Weiner, *Z. Phys. C* **9**, 271 (1981).
- [35] S. Chakrabaty, S. Raha, and B. Sinha, *Phys. Lett. B* **229**, 112 (1989).
- [36] O. G. Benvenuto and G. Lugones, *Phys. Rev. D* **51**, 1989 (1995).
- [37] G. X. Peng, H. C. Chiang, J. J. Yang, L. Li, and B. Liu, *Phys. Rev. C* **61**, 015201 (1999).
- [38] G. X. Peng, H. C. Chiang, B. S. Zou, P. Z. Ning, and S. J. Luo, *Phys. Rev. C* **62**, 025801 (2000).
- [39] X. J. Wen, X. H. Zhong, G. X. Peng, P. N. Shen, and P. Z. Ning, *Phys. Rev. C* **72**, 015204 (2005).
- [40] G. X. Peng, U. Lombardo, and A. Li, *Phys. Rev. C* **77**, 065807 (2008).
- [41] C. J. Xia, G. X. Peng, S. W. Chen, Z. Y. Lu, and J. F. Xu, *Phys. Rev. D* **89**, 105027 (2014).
- [42] R. X. Xu, *Astrophys. J.* **596**, L59 (2003); *Int. J. Mod. Phys. D* **19**, 1437 (2010).
- [43] K. Schertler, C. Greiner, and M. H. Thoma, *Nucl. Phys. A* **616**, 659 (1997).
- [44] M. I. Gorenstein and S. N. Yang, *Phys. Rev. D* **52**, 5206 (1995).
- [45] B. A. Freedman and M. McLerran, *Phys. Rev. D* **16**, 1130 (1977); **16**, 1147 (1977); **16**, 1169 (1977); **17**, 1109 (1978).
- [46] V. Baluni, *Phys. Rev. D* **17**, 2092 (1978).
- [47] T. Toimela, *Int. J. Theor. Phys.* **24**, 901 (1985); **26**, 1021 (1987).
- [48] C. Alcock, E. Farhi, and A. V. Olinto, *Astrophys. J.* **310**, 261 (1986).
- [49] P. Haensel, J. L. Zdunik, and R. Schaeffer, *Astron. Astrophys.* **160**, 121 (1986).
- [50] E. S. Fraga and R. D. Pisarski, *Phys. Rev. D* **63**, 121702(R) (2001).
- [51] E. S. Fraga and P. Romatschke, *Phys. Rev. D* **71**, 105014 (2005).
- [52] E. S. Fraga, *Nucl. Phys. A* **774**, 819 (2006).
- [53] A. Kurkela, P. Romatschke, and A. Vuorinen, *Phys. Rev. D* **81**, 105021 (2010).
- [54] G. X. Peng, *Europhys. Lett.* **72**, 69 (2005).
- [55] K. Schertler, C. Greiner, and M. H. Thoma, *J. Phys. G* **23**, 2051 (1997).
- [56] X. J. Wen, Z. Q. Feng, N. Li, and G. X. Peng, *J. Phys. G* **36**, 025011 (2009).
- [57] X. J. Wen, J. Y. Li, J. Q. Liang, and G. X. Peng, *Phys. Rev. C* **82**, 025809 (2010).
- [58] X. J. Wen, S. Z. Su, D. H. Yang, and G. X. Peng, *Phys. Rev. D* **86**, 034006 (2012).
- [59] J. F. Xu, G. X. Peng, Z. Y. Lu, and S. S. Cui, *Sci. China Phys. Mech. Astron.* **58**, 042001 (2015).
- [60] T. van Ritbergen, J. Vermaseren, and S. Larin, *Phys. Lett. B* **400**, 379 (1997).
- [61] K. G. Chetyrkin, B. A. Kniehl, and M. Steinhauser, *Phys. Rev. Lett.* **79**, 2184 (1997).
- [62] W. E. Caswell, *Phys. Rev. Lett.* **33**, 244 (1974).
- [63] K. A. Olive *et al.* (Particle Data Group), *Chin. Phys. C* **38**, 090001 (2014).
- [64] P. S. Ray, D. Chakrabarty, C. A. Wilson-Hodge, B. F. Philips, R. A. Remillard, A. M. Levine, K. S. Wood, M. T. Wolff, C. S. Gwon, T. E. Strohmayer *et al.*, *Proc. SPIE* **7732**, 773248 (2010).
- [65] M. Feroci and T. L. Consortium, *Exp. Astron.* **34**, 415 (2012).
- [66] A. Watts, R. Xu, C. Espinoza, N. Andersson, J. Antoniadis, D. Antonopoulou, S. Buchner, S. Dai, P. Demorest, P. Freire *et al.*, *Proc. Sci.*, AASKA14 (2015) 043 [arXiv: 1501.00042].
- [67] Z. Arzumanyan, K. C. Gendreau, C. L. Baker, T. Cazeau, P. Hestnes, J. W. Kellogg, S. J. Kenyon, R. P. Kozon, K. C. Liu, S. S. Manthripragada *et al.*, *Proc. SPIE* **9144**, 914420 (2014).
- [68] M. Prakash, I. Bombaci, M. Prakash, P. J. Ellis, J. M. Lattimer, and J. M. Knorren, *Phys. Rep.* **280**, 1 (1997).
- [69] J. Antoniadis, P. C. C. Freire, N. Wex *et al.*, *Science* **340**, 1233232 (2013).
- [70] P. B. Demorest, T. Pennucci, S. M. Ransom, M. S. E. Roberts, and J. W. T. Hessels, *Nature (London)* **467**, 1081 (2010).
- [71] Z. Roupas, *Phys. Rev. D* **91**, 023001 (2015).
- [72] M. Buballa, V. Dexheimer, A. Drago, E. Fraga, P. Haensel, I. Mishustin, G. Pagliara, J. Schaffner-Bielich *et al.*, *J. Phys. G* **41**, 123001 (2014).
- [73] H. Heiselberg and M. Hjorth-Jensen, *Phys. Rep.* **328**, 237 (2000).
- [74] M. Herzog and F. K. Ropke, *Phys. Rev. D* **84**, 083002 (2011).
- [75] G. X. Peng, X. J. Wen, and Y. D. Chen, *Phys. Lett. B* **633**, 314 (2006).
- [76] M. Angeles Perez-Garcia, J. Silk, and J. R. Stone, *Phys. Rev. Lett.* **105**, 141101 (2010).
- [77] V. M. Lipunov, *Astrophysics of Neutron Stars* (Springer-Verlag, Berlin, 1992), p. 30.
- [78] M. G. Alford, K. Rajagopal, and F. Wilczek, *Nucl. Phys. B* **537**, 433 (1999).
- [79] M. Huang and I. A. Shovkovy, *Phys. Rev. D* **70**, 051501 (2004).
- [80] R. C. Duncan and C. Thompson, *Astrophys. J.* **392**, L9 (1992).
- [81] E. J. Ferrer, V. de la Incera, and C. Manuel, *Phys. Rev. Lett.* **95**, 152002 (2005); *Nucl. Phys. B* **747**, 88 (2006).
- [82] V. Dexheimer, D. P. Menezes, and M. Strickland, *J. Phys. G* **41**, 015203 (2014).
- [83] D. F. Hou, H. Liu, and H. C. Ren, *Phys. Rev. D* **86**, 121703R (2012).
- [84] K. Xiao, F. Liu, and F. Q. Wang, *Phys. Rev. C* **87**, 011901 (2013).
- [85] G. X. Peng, *Phys. Lett. B* **634**, 413 (2006).